scientific reports

Check for updates

OPEN

Stationarity assessment of resting state condition via permutation entropy on EEG recordings

Alessio Perinelli[1,2]✉ & Leonardo Ricci[1,3]✉

The analysis of electrophysiological recordings of the human brain in resting state is a key experimental technique in neuroscience. Resting state is the default condition to characterize brain dynamics. Its successful implementation relies both on the capacity of subjects to comply with the requirement of staying awake while not performing any cognitive task, and on the capacity of the experimenter to validate that compliance. Here we propose a novel approach, based on permutation entropy, to assess the reliability of the resting state hypothesis by evaluating its stability during a recording. We combine the calculation of permutation entropy with a method to estimate its uncertainty out of a single time series. The approach is showcased on electroencephalographic data recorded from young and elderly subjects and considering eyes-closed and eyes-opened resting state conditions. Besides highlighting the reliability of the approach, the results show higher instability in elderly subjects, hinting at qualitative differences between age groups in the distribution of unstable brain activity. The method can be applied to other kinds of electrophysiological data, like magnetoencephalographic recordings. In addition, provided that suitable hardware and software processing units are used, the implementation of the method can be translated into a real time one.

The characterization of brain states by relying on the analysis of electrophysiological recordings is a fundamental issue in neuroscience and a basic tool in the medical practice. Among the possible brain states, the so-called resting state plays a major role in the investigation of brain functional organization[1]. The interest in resting state brain dynamics was first prompted by Biswal et al.[2] in the context of functional magnetic resonance imaging (MRI). Since then, the resting state paradigm has been widely used also in connection with electroencephalographic (EEG) and magnetoencephalographic (MEG) analytical techniques[3–5]. A well-known result concerning the brain organization in resting state is provided by the identification, primarily via functional MRI, of resting state networks[6,7]. Among these, the "default mode" network is possibly the most studied one[8,9].

The definition of the resting state condition is procedural: typically, resting state corresponds to subjects being instructed by an operator to "do nothing", i.e. not to perform any cognitive task, while either keeping their eyes closed or fixating a static marker on a screen. Once the instruction is provided, the subject is entrusted with its implementation. As a matter of fact, the operator does not have more than trust to depend on in order to establish the reliability of the outcome of an experiment. How to objectively determine the quality of the resting state implementation is an unsolved issue. Two different approaches can be envisaged. A first possibility is to devise rigorous and reproducible protocols to be followed when conducting resting state experiments[10]. Indeed, as some researchers have pointed out[11,12], a lack of a shared consensus on the implementation of a resting state is a possible reason for the ongoing underutilization of resting state measurements in clinical applications. However, regardless of how meticulously it is implemented, a protocol cannot provide any *a posteriori* assessment of the reliability of recorded data. Conversely, the second approach consists of assessing the stability of resting state by means of a measurable quantity. This strategy was followed, for example, by using graph metrics in order to evaluate the reliability of resting state brain networks identified through functional MRI[13].

The goal of the present paper is to develop a technique to evaluate the stationarity of a system ahead of—and setting constraints to—any further, field-specific analysis. As a major application case, we address the problem of stability of the resting state assumption by analyzing segments of EEG time series to detect variations in the dynamical state of the brain. To this purpose, permutation entropy[14] (PE) is used as a marker of time series complexity. Among approaches typical of information theory to carry out advanced, nonlinear analysis of EEG recordings, PE has recently become increasingly popular thanks to the simplicity of implementation[15]: PE was

[1]Department of Physics, University of Trento, Trento 38123, Italy. [2]INFN-TIFPA, University of Trento, Trento 38123, Italy. [3]CIMeC, Center for Mind/Brain Sciences, University of Trento, Rovereto 38068, Italy. ✉email: alessio.perinelli@unitn.it; leonardo.ricci@unitn.it

proposed, for example, as a mean to automatically detect epileptic seizure[16] and as a biomarker for Alzheimer's disease[17]. The technique might be used as an additional component of a quality control protocol[18,19].

The approach proposed here addresses a different issue with respect to the so-called "test-retest reliability" of electrophysiological measurements[20]. In this latter approach, two sessions separated in time by a few days up to a few years are used to evaluate the stability of a given measure, such as source current density estimates[21] or spectral and fractal properties derived from EEG data[22]. More recently, the reliability of sessions time separated by one week was investigated on measures of spectral power, functional connectivity and brain "microstates"[23]. Our approach instead concerns recordings within the very same session, whereby nonstationarity can emerge due to short-term phenomena, such as fatigue, that are undetectable when comparing separate sessions.

The data considered here are EEG recordings of healthy young and elderly subjects and reconstructed at a set of brain locations. Data are extracted from the LEMON public database[24], in which resting state EEG recordings are available both in eyes-closed (EC) and eyes-opened (EO) conditions. The availability of several interleaved EC-EO segments for each subject provided the necessary segmentation to evaluate resting state stability. Although one might argue that alternating EC-EO states violates the pure resting state assignment, the simplicity of the task is not expected to affect the resting state condition, while avoiding mental drifts like falling asleep or boredom.

The analysis proposed here is carried out by evaluating PE on different segments under the null hypothesis of its constancy during the whole recording in each one of the two conditions. The analysis immediately calls for the necessity of estimating the uncertainty of PE assessments. To this purpose, we relied on a recently developed technique[25] that allows for overcoming the problem of each time series being a singleton. In the final step of the analysis, a chi-square test is used to determine the statistical significance of the stationarity hypothesis. These features underpin the novelty and robustness of the approach introduced here, whose scope is not limited to neuroscience. Indeed, the method discussed here is useful in any field where it is necessary to detect nonstationarity of a system's dynamics out of time series. In this sense, the procedure described in the present work can be implemented as a "stationarity test" prior to any analysis pipeline: the detection of nonstationarity—e.g. in brain recordings in terms of resting-state instability—could be used as a filter to check the quality of the analyzed data, or as a preliminary information in order to choose between different analysis methods.

Assessing the stability of the resting state

The dataset considered here corresponds to two sets of subjects: a "young" set of 30 healthy subjects in the age range between 20 and 35 years old, and an "elderly" set of 30 healthy subjects in the age range between 60 and 80 years old. For each subject, we extracted sequences of current dipole power reconstructed at 30 brain locations, henceforth referred to as "nodes". Each sequence consists of 12 segments, six corresponding to the EC condition and six to the EO condition, whereas the two conditions are interleaved. Each segment instead consists of 15000 samples that, due to the 250 Hz sampling frequency, cover a time interval of 60 s. Details of the sequence extraction and the related preprocessing are provided in the Methods section. The total number of time series analyzed is $(30+30)\times 30\times 12 = 21600$. For each subject, node and condition, six values of PE and the related uncertainty are estimated by means of the steps also described in the Methods section. The permutation dimension $m = 7$ was chosen as a trade-off between resolution capability and computational affordability. In the Methods section we also discuss the effect of choosing a different dimension and, in addition, a different sampling frequency.

Figure 1 shows an example for a single subject belonging to the young group and a single node. Stability is assumed to occur whenever PE is independent of time, i.e. fluctuations of PE between segments are statistically compatible with the uncertainty associated to the PE values. The stability of the resting state is then evaluated for each of the two sets (EC and EO) of six PE assessments as follows. A constant value $\hat{h}$, corresponding to a horizontal line in the plot, is fitted to the data. The p-value corresponding to the resulting χ^2 statistic is then evaluated by relying on a χ^2 distribution with 5 degrees of freedom. Consequently, given a subject, node and

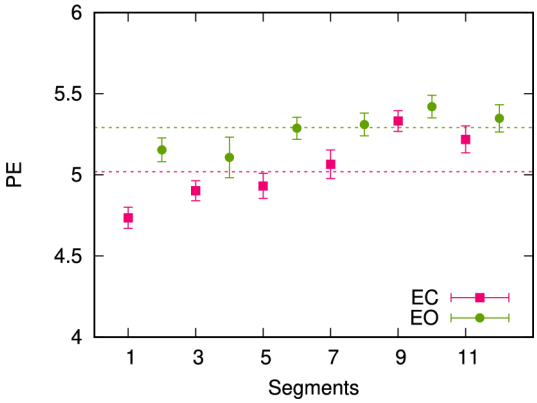

Fig. 1. Example, for a single subject, of the resting state stability analysis. The dashed lines correspond to the constant $\hat{h}$ fitted to the two sets (EC and EO) of PE values. As explained in the main text, the EC condition (red squares) is unstable, whereas the EO condition (green dots) is stable.

condition, resting state is deemed to be "stable" ("unstable") if the p-value overcomes (is less than) the Bonferroni-corrected significance threshold of $0.05/30 \simeq 0.0017$.

The values of the best-fit constant $\hat{h}$ for the EC and EO conditions are equal to 5.0 ± 0.1 and 5.29 ± 0.04 , respectively. The χ^2 test provides, for the two conditions, p-values equal to $2 \cdot 10^{-10}$ and 0.087, leading to the conclusion that resting state under the EC condition is unstable, whereas stability occurs under the EO condition.

Stability analysis in terms of age, condition, and brain region

The results of the stationarity assessment are displayed in Fig. 2 for young subjects, and Fig. 3 for elderly subjects. Each figure shows a color map of stability as a function of subject and node. Specifically, to each subject-node pair, a different color is assigned depending on stability: white color if both EO and EC are deemed to be stable; light green for unstable EC; bluish green for unstable EO; dark purple for both unstable EC and EO. Moreover, on top of the color maps, a histogram shows, for each node, the number of subjects for which that node is deemed to be "unstable" in either the EC or EO condition. In the top panel histogram for each node two bars are present, one corresponding to the count of EC unstable pixels and one to the count of EO unstable pixels. In this way, (in-)stability is averaged across all subjects belonging to the same age group.

The data displayed in Figs. 2 and 3 suggest that "instability" of resting state is not uncommon: the number of subjects in which an "unstable" resting state condition is detected is close to one third of the whole set of subjects. Averaging on the 30 nodes, the frequency of unstable nodes for the young group is $\simeq 26\%$ (EC) and $\simeq 28\%$ (EO), while for the elderly group it is equal to $\simeq 44\%$ (EC) and $\simeq 34\%$ (EO). In other words, the number of subjects exhibiting "instability" is generally larger for the elderly group than for the young group, regardless of the brain location. This observation can be explained by elderly subjects tending to be more affected by fatigue.

The smaller panel to the right of each color map reports a histogram of the number of subjects as a function of the number of stable nodes. For each age group, this histogram provides a pooled assessment of reliability. While the distribution for young subjects is right-skewed, with most subjects having a number of stable nodes $\gtrsim 20$, the distribution for elderly subjects appear to be more noisy, with the majority of subjects exhibiting either a "globally stable" or a "globally unstable" resting state. This observation might reflect an underlying lower modularity in elderly subjects[26], namely the fact that brain dynamics tends to involve many areas.

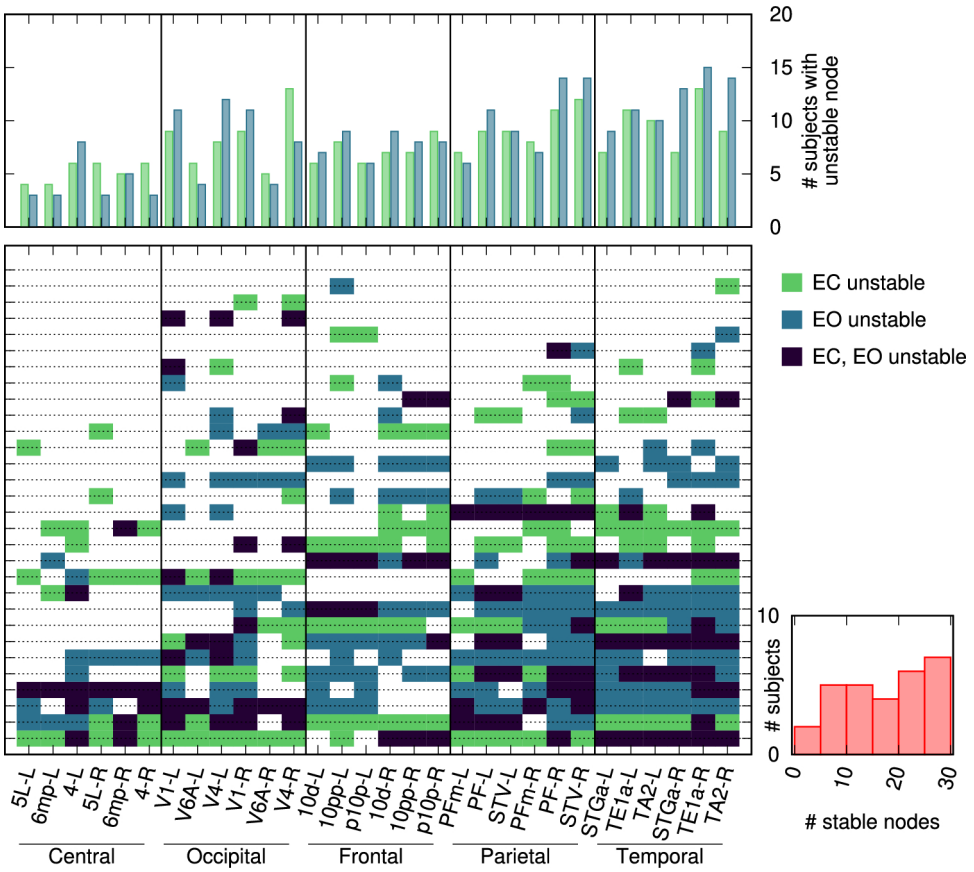

Fig. 2. Stationarity assessment results for the set of young subjects. The color map shows subject-node stability: each row corresponds to a subject, ordered by increasing number of stable nodes (from bottom to top). The top panel histogram corresponds to the number of subjects for which a given node is deemed to be unstable under the EC or EO condition. The bottom-right red histogram displays the distribution of the number of stable nodes.

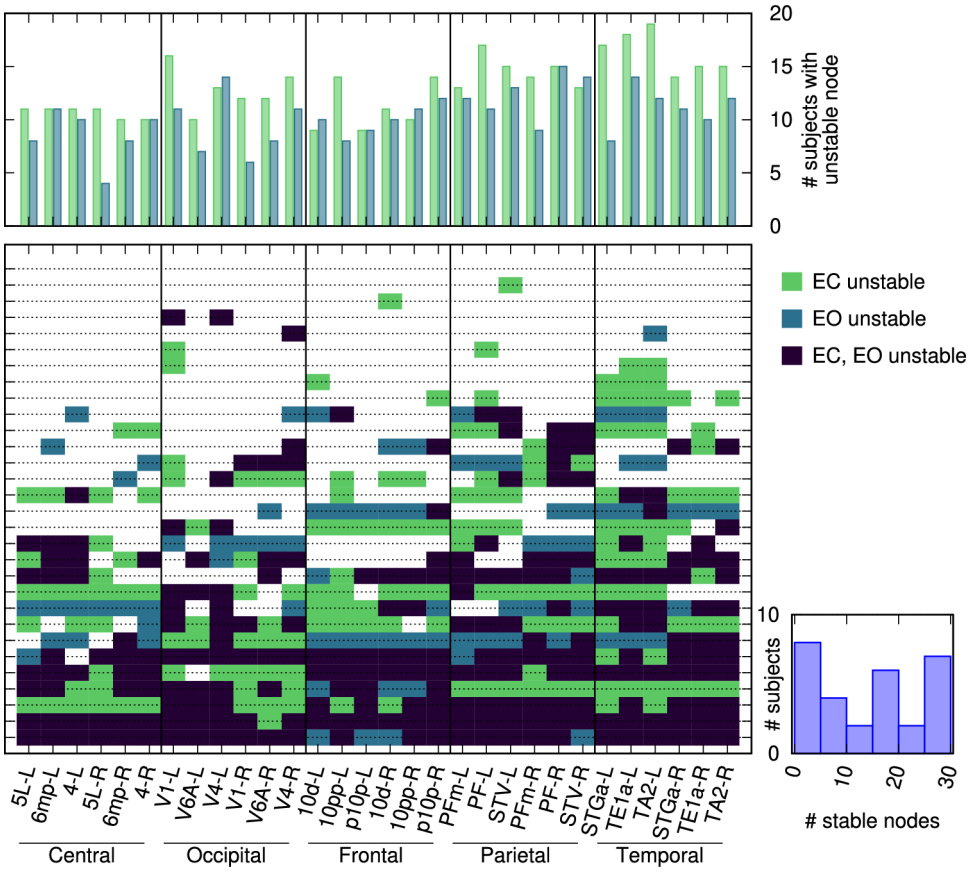

Fig. 3. Stationarity assessment results for the set of elderly subjects. The color map shows subject-node stability: each row corresponds to a subject, ordered by increasing number of stable nodes (from bottom to top). The top panel histogram corresponds to the number of subjects for which a given node is deemed to be unstable under the EC or EO condition. The bottom-right blue histogram displays the distribution of the number of stable nodes.

Complexity of stable resting states

Whenever a combination of subject, node and condition is deemed to be stable, the corresponding $\hat{h}$ value, which is indeed an average PE, can be taken as a marker to characterize the complexity of the underlying dynamics. The distributions of $\hat{h}$ values corresponding to stable resting state are shown in Fig. 4, grouped by age and condition. It is first worth highlighting that the maximum PE value with $m = 7$, corresponding to white noise time series, is $\ln 7! \simeq 8.525$: according to the data shown in Fig. 4, the EEG recordings analyzed here do not correspond to a purely stochastic dynamics.

The four distributions displayed in Fig. 4 are comparable in width and shape, though with a slight shift towards higher PE values occurring in the elderly sets.

To quantify possible differences due to age, condition or brain area in the PE values corresponding to "stable" resting state, we set up a three-way ANOVA followed by a post-hoc test on significant effects. The significance level was set to 0.05. Data were factored by age (young, elderly), condition (EC, EO) and brain region (central, occipital, frontal, parietal, temporal). Each group contains between 82 and 155 values (120 on average). The three-way ANOVA, implemented in R[27], returned a significant main effect ($p < 0.001$) for all three factors. We refrain from considering interaction effects, as such a detailed analysis goes beyond the scope of the present work.

As far as age is concerned, the post-hoc test revealed a significantly higher PE for elderly subjects, possibly implying a more noisy activity. On the other hand, the EO condition turns out to correspond to a higher PE with respect to the EC condition. These two observations are indeed in line with a qualitative conclusion that can be drawn from Fig. 4. Regarding the significant effect of the brain area factor, the post-hoc test reveals that each area provides a significantly different PE values with respect to the others, except for the central-occipital pair. Taking into account the sign of these differences, one can order the brain areas from the lowest to the highest PE value, i.e. from the one exhibiting a more ordered dynamics to the one being more noise-like: central and occipital; parietal; temporal; frontal. To provide a visual reference for the latter result, the data of Fig. 4 are plotted in Fig. 5 grouped by area, rather than age and condition.

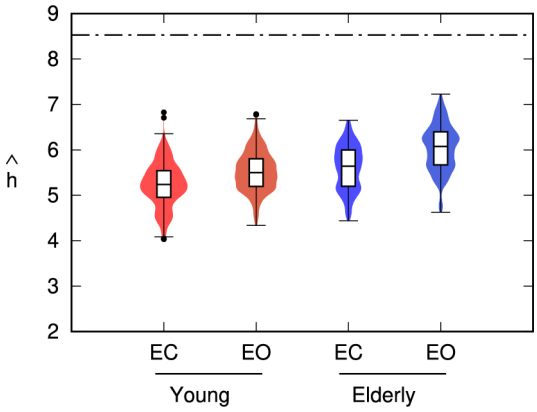

Fig. 4. Distribution plots of the values of $\hat{h}$ corresponding to a "stable" resting state for the young-elderly and EC-EO groupings. The dash-dotted line corresponds to the maximum PE value for $m = 7$, namely $\ln 7! \simeq 8.525$. The number of $\hat{h}$ values contributing to each distribution are, from left to right: 643, 645, 507, 591.

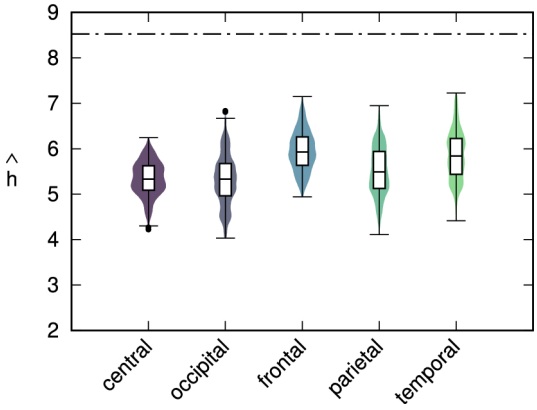

Fig. 5. Distribution plots of the values of $\hat{h}$ corresponding to a "stable" resting state grouped by brain area. The dash-dotted line corresponds to the maximum PE value for $m = 7$, namely $\ln 7! \simeq 8.525$. The number of $\hat{h}$ values contributing to each distribution are, from left to right: 549, 486, 503, 442, 426.

Discussion

By virtue of a surrogate-based technique for the estimation of PE uncertainty[25], here we proposed a novel approach to assess the stationarity of recorded time series. We showcased the approach by evaluating the stability of resting state and by exploiting, as a benchmark, the EC-EO conditions. While the use of PE was described in the scientific literature, for example, to classify sleep stages[28] and pathological[29] or drug-induced conditions[30], wake, healthy resting state recordings have obtained less attention[31].

The EC-EO paradigm is typically studied in terms of the spectral changes, most notably the presence of alpha rhythms in EC[32]. More recently, the EC-EO paradigm was analyzed through an information-theoretic approach in two works, which found similar results to the one presented here in terms of PE differences between conditions. In the first one[33], the authors analyzed EEG recordings under the two conditions by applying a method[34] aimed at assessing the transition probabilities of ordinal patterns (i.e. permutations) and determining the so-called network-averaged node entropy and asymmetry coefficient. The authors showed that the EO condition is characterized by higher entropy values, accompanied by a lower asymmetry coefficient, with respect to the EC condition. In the second paper[35] the authors described an approximate entropy analysis of EEG recordings recorded in the two conditions, again showing that the EO condition provides higher entropy values than the EC. Those results are in agreement with the ones obtained with the present analysis: we also found higher PE values in the EO condition.

It is worth remarking that the works mentioned above carried out the respective analyses in sensor space: while this approach is computationally less demanding, one has to keep in mind that the influence of volume conduction might produce spurious results, as it was shown in the case of connectivity measures[36,37]. While the present method could be applied to sensor space data as well, the reconstruction of source activity enhances the interpretability of the results: assuming that stability is a property of the system (sources) rather than the

instrument (sensor), the assessment turns out to be more robust and its interpretation in terms of underlying brain dynamics is more immediate.

PE is a well-established complexity quantifier capable of detecting dynamical changes in time series[38] by virtue of its definition depending on a weak stationarity assumption[14]. The use of PE in neuroscience has acquired in the last decades an increasingly relevant role[15,39,40]. The most relevant clinical application of PE is its being a promising biomarker[41] for the early diagnosis of cognitive diseases, most notably mild cognitive impairment and Alzheimer's disease[17,42]. A potential clinical use of PE was also explored in the context of traumatic brain injury[43], as well as to predict epileptic seizures[44–46] and to measure the effect of anaesthetic drugs[47]. Within the context of neuroscience, the approach presented here provides a statistically robust way to investigate stability of resting state, which might be used as a biomarker to distinguish healthy and pathological conditions out of EEG recordings. This application, which would be of major clinical interest, is beyond the scope of the present work and would call for dedicated randomized studies.

The studies referenced above have a common limitation, namely the fact that the application of information-theoretical tools to electrophysiological data is often lacking an estimation of the related uncertainty, despite the availability of asymptotic formulas[48,49]: the significance of the quantities inferred in the analysis is typically based on averaging over a set of subjects. Conversely, the approach followed here, which relies on surrogate-based estimation of PE uncertainty, is capable of assigning an uncertainty value to each PE assessment. This capability paves the way to the possibility of drawing subject-specific quantitative conclusions from data. This possibility is crucial, as attested by the significant between-subject variability of the present results. As it is clearly visible from Figs. 2, 3, the stability of a specific node is non-trivially dependent on the subject. Such variability, which is typical of neuroscientific data, further highlights the need for quality control approaches that can be applied subject-wise, rather than on an averages across subjects. Besides the present application to assess the stability of the resting state condition, the possibility of drawing quantitative conclusions on single subjects is of primary importance in the development of diagnostic biomarkers based on EEG measures[50] and other kinds of electrophysiological data like, for example, magnetoencephalographic recordings.

The present study is, to our knowledge, the first one to address the issue of a stationary behavior of nodes by means of permutation entropy. Future developments might regard the application of the method to more challenging neuroscientific contexts, as well as to investigate the link of stability with other brain observables and its role in the brain function.

As final remarks, it is worth noting that a real time implementation of the method just depends on the hardware and software units that are used to process data. In addition, the method proposed in the present work is not limited to neuroscience: its scope can be widened to include any field where it is necessary to detect nonstationarity of a system's dynamics out of singleton time series.

Methods

Dataset and preprocessing

EEG data used in the present work belong to the Leipzig Mind-Brain-Body "LEMON" database[24], which is publicly available[51]. Data were recorded in compliance with the Declaration of Helsinki and the related study protocol was approved by the ethical committee at the University of Leipzig (reference number 154/13-ff, see also the related data publication[24]). The available raw recordings were acquired in a sound-attenuated EEG booth by means of a 62-channels active ActiCAP EEG device whose electrodes were attached according to the international standard 10-20 system. The corresponding signals are digitized with a sampling rate of $2.5\,\mathrm{kHz}$ upon bandpass-filtering them between $0.015\,\mathrm{Hz}$ and $1\,\mathrm{kHz}$. Further details on the data acquisition protocol are available in a dedicated publication[24]. Two sets of subjects are considered: 30 "young" healthy subjects in the age range between 20 and 35 years old (19 males, 11 females), and 30 "elderly" healthy subjects in the age range between 60 and 80 years old (19 males, 11 females).

Data preprocessing and source reconstruction procedure are described in detail in two previous works[26,52]. For the sake of clarity, we summarize here the key steps. Raw EEG recordings were first filtered within the frequency band between $0.1\,\mathrm{Hz}$ and $40\,\mathrm{Hz}$ by relying on fourth-order high-pass and low-pass filters; however, due to the low-pass filter still having at $50\,\mathrm{Hz}$ an attenuation of $\simeq 16\,\mathrm{dB}$ corresponding to a factor $\simeq 0.15$, the power line frequency at $50\,\mathrm{Hz}$ was suppressed by means of a notch filter having a width of $\sim 1\,\mathrm{Hz}$; third, the sampling frequency was reduced to $250\,\mathrm{Hz}$ by downsampling the data. The choice of setting a sampling rate of $250\,\mathrm{Hz}$ stems from the fact that, for PE to be reliably assessed (see next section), the sampling period has to match the typical time scale of the observed dynamics: in the present case, the oscillations due to brain dynamics are of order $\lesssim 100\,\mathrm{Hz}$. Higher sampling rates introduce redundancy in the data, in terms of higher occurrence rates of identical consecutive patterns; lower sampling rates produce instead noise-like uncorrelated data. Artifacts due to cardiac, muscular and eye activity were removed by relying on an independent component analysis. To carry out source reconstruction, head models were built out of the individual MRI scans provided in the LEMON database. Source activity was reconstructed by means of the exact low-resolution electromagnetic tomography algorithm ("eLoreta") that provided current dipoles with unconstrained orientations on a 10 mm template grid. The extracted sequences correspond to current dipole power reconstructed at 30 brain locations, or "nodes", selected as the centroids of 30 brain regions among the 360 defined in the atlas by Glasser et al.[53]. The regions considered are V1, V6A, V4 (occipital); 4, 5L, 6mp (central); Pfm, PF, STV (parietal); STGa, TE1a, TA2 (temporal); 10d, 10pp, p10p (frontal); each region was selected symmetrically in both hemispheres.

Each EEG acquisition run consists of 16 alternated segments in EC (8 segments) and EO (8 segments) conditions. To reduce transient effects, we selected 12 consecutive segments, namely 6 EC and 6 EO, by discarding the first two and the last two segments of each run. Each raw segment covers between $\gtrsim 60\,\mathrm{s}$ and $90\,\mathrm{s}$: with the same purpose of reducing transients, we trimmed each segment to $60\,\mathrm{s}$, corresponding to 15000 samples, by symmetrically removing the leading and trailing data points. In principle, one might want to evaluate PE on

shorter segments in order to minimize the effect of nonstationary behaviors. However, a lower bound to the length of the time series over which PE can be reliably evaluated is set by the permutation order and thus by the number of possible symbolic sequences: in the present case, $m = 7$ (see next section), so the number of samples within a segment should be significantly larger than $m! = 5040$. Also due to the fact that many symbolic sequences do not occur, the chosen length of 15000 appears to be adequate.

Permutation entropy

To compute PE, m-dimensional trajectories y_n are constructed by selecting m consecutive elements from a scalar time series $Y = \{y_n\}$: $\mathrm{y}_n = (y_n, y_{n+1}, \ldots, y_{n+m-1})$. A trajectory is then encoded into a permutation $(s_{n,1}, \ldots, s_{n,m})$, were $s_{n,j}$ are integer numbers each corresponding to the rank of y_{n+j-1} within the trajectory y_n. As the permutation elements $s_{n,j}$ belong to the range $[1, m]$, the number of possible permutations is $m!$. For each possible permutation, the observed rate $\hat{p}_S$ is assessed as the occurrence frequency of that permutation. PE is finally estimated out of the observed rates $\hat{p}_S$ according to the following expression:

$$\hat{H}_m(Y) = -\sum_S (\hat{p}_S \ln \hat{p}_S) + \frac{\hat{M} - 1}{2(N - m + 1)},$$

where the sum corresponds to the so-called plug-in estimator, while the second term is the Miller-Madow correction[48,54] that compensates the plug-in estimator bias and depends on the time series length N and the number $\hat{M}$ of observed permutations ($\hat{M} \leqslant m!$). (We henceforth assume that $0 \ln 0 = 0$).

The growth rate of PE with the dimension m corresponds, asymptotically, to the Kolmogorov-Sinai (KS) entropy of the underlying source. However, because the number of possible permutations grows as $m!$, the evaluation of PE for $m \gtrsim 10$, and thus of the KS entropy, is often impractical for computational reasons. Consequently, PE is instead typically employed at fixed m as a marker of complexity or—as in the present work—to detect nonstationarity by evaluating it on different segments of a time series[38]. In this context, the demand of a large m has to be traded off against the fact that an unbiased estimation of PE requires the length of the input time series to be much larger than the number of observed permutations. The analysis discussed here was carried out by considering trajectories having dimension $m = 7$.

Permutation entropy uncertainty estimation

A key requirement of the analysis discussed in the present work is the estimation of the uncertainty associated to each PE assessment. To this purpose, we apply a recently developed method[25] that relies on the construction of a set of proxy time series out of the original one via surrogate generation[55]. Specifically, the surrogate generation algorithm used here is the iterative amplitude-adjusted Fourier transform (IAAFT) algorithm[56,57], whereby the amplitude distribution and the (approximate) autocorrelation of the original time series are preserved in the surrogate ones. Upon generating a number L of surrogate time series and computing the corresponding PE values, the uncertainty on the PE of the original time series is provided by the standard deviation of the L surrogate PE assessments multiplied times a suitably trimmed scaling factor α. As it was shown therein, a robust choice for the scaling factor, which is henceforth adopted, is $\alpha = 2$. The number of surrogate time series to be generated for each evaluation was set to $L = 100$, which is computationally affordable while providing a sufficiently accurate evaluation of the PE uncertainty.

Dependence of permutation entropy on dimension and lag

In this section we analyze the effect of the choice of partition dimension and of the sampling frequency. Figure 6a shows a scatter plot of PE evaluated with $m = 7$ versus $m = 6$ and normalized to the respective maximum value $\ln(m!)$. The plot contains 21600 points, each corresponding to a single time series. The correlation between the two evaluations is apparent. However, the values with $m = 7$ are slightly less than the respective values with $m = 6$, which hints at a higher information resolution for $m = 7$.

Similarly, Fig. 6b shows a scatter plot of PE evaluated with $m = 6$, $L = 2$ versus $m = 6$, $L = 1$ and normalized to the maximum value $\ln(6!)$. The $L = 2$ values are obtained by downsampling the time series by a factor 2. Again, the correlation is apparent with, however, an upward offset for the $L = 2$ assessment as compared to the respective $L = 1$, which is due to the loss of regularity as a consequence of the downsampling. For higher values of PE the offset "saturates" towards the maximum normalized value equal to 1.

One might argue whether an higher value of m, for example $m = 8$, would further improve the quality of the analysis. However, one has to cope with the length of the time series, which has to overcome the number of possible permutations (approximately 40000 for $m = 8$).

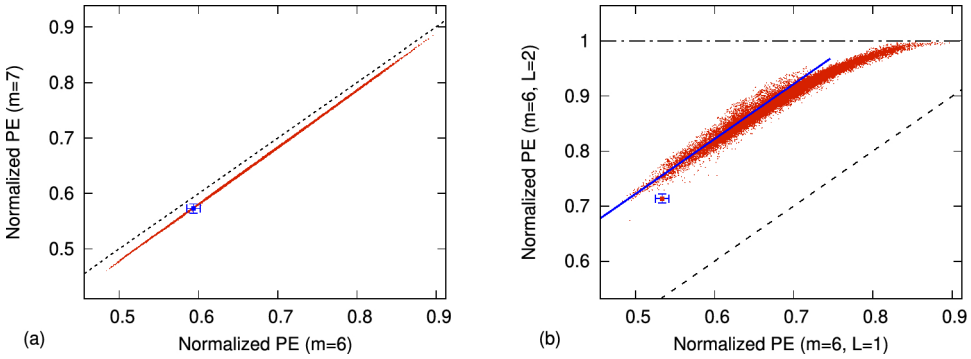

Fig. 6. (**a**) Scatter plot of PE evaluated with $m = 7$ versus $m = 6$ on the 21600 time series. The PE is normalized on the respective maximum value $\ln(m!)$, with $m = 6, 7$. The average value of the uncertainty on the PE assessments are displayed on a single point (blue) by means of two error bars equal to 0.0085 ($m = 6$) and 0.0084 ($m = 7$). The black, dashed line corresponds to a straight line going through the origin and having unitary slope. (**b**) Scatter plot of PE evaluated with $m = 6$, $L = 2$ versus $m = 6$, $L = 1$ on the 21600 time series. The PE is normalized on the maximum value $\ln(6!)$. The average value of the uncertainty on the PE assessments are displayed on a single point (blue) by means of two error bars equal to 0.0085 ($L = 1$) and 0.0079 ($L = 2$). The black, dashed line corresponds to a straight line going through the origin and having unitary slope. The blue, solid line corresponds to a straight line having unitary slope and an offset at the origin equal to 0.22 that was evaluated by fitting the straight line to the points with abscissa < 0.6.

Data availability

Raw EEG recordings used in the present work are available in the LEMON database at Ref.[51]https://fcon_1000.projects.nitrc.org/indi/retro/MPI_LEMON.html.

Received: 10 July 2024; Accepted: 2 December 2024
Published online: 03 January 2025

References

1. Raichle, M. E. et al. A default mode of brain function. *Proc. Natl. Acad. Sci.* **98**, 676–682. https://doi.org/10.1073/pnas.98.2.676 (2001).
2. Biswal, B., Zerrin Yetkin, F., Haughton, V. M. & Hyde, J. S. Functional connectivity in the motor cortex of resting human brain using echo-planar MRI. *Magn. Reson. Med.* **34**, 537–541. https://doi.org/10.1002/mrm.1910340409 (1995).
3. van Diessen, E. et al. Opportunities and methodological challenges in EEG and MEG resting state functional brain network research. *Clin. Neurophysiol.* **126**, 1468–1481. https://doi.org/10.1016/j.clinph.2014.11.018 (2015).
4. Perinelli, A., Chiari, D. E. & Ricci, L. Correlation in brain networks at different time scale resolution. *Chaos* **28**, 063127. https://doi.org/10.1063/1.5025242 (2018).
5. Perinelli, A., Tabarelli, D., Miniussi, C. & Ricci, L. Dependence of connectivity on geometric distance in brain networks. *Sci. Rep.* **9**, 13412. https://doi.org/10.1038/s41598-019-50106-2 (2019).
6. Fox, M. D. & Raichle, M. E. Spontaneous fluctuations in brain activity observed with functional magnetic resonance imaging. *Nat. Rev. Neurosci.* **8**, 700–711. https://doi.org/10.1038/nrn2201 (2007).
7. Thomas Yeo, B. T. et al. The organization of the human cerebral cortex estimated by intrinsic functional connectivity. *J. Neurophysiol.* **106**, 1125–1165. https://doi.org/10.1152/jn.00338.2011 (2011).
8. Buckner, R. L., Andrews-Hanna, J. R. & Schacter, D. L. The brain's default network. *Ann. N. Y. Acad. Sci.* **1124**, 1–38. https://doi.org/10.1196/annals.1440.011 (2008).
9. de Pasquale, F. et al. Temporal dynamics of spontaneous MEG activity in brain networks. *Proc. Natl. Acad. Sci.* **107**, 6040–6045. https://doi.org/10.1073/pnas.0913863107 (2010).
10. Caeyenberghs, K. et al. ENIGMA's simple seven: Recommendations to enhance the reproducibility of resting-state fMRI in traumatic brain injury. *NeuroImage Clin.* **42**, 103585. https://doi.org/10.1016/j.nicl.2024.103585 (2024).
11. Lv, H. et al. Resting-state functional MRI: Everything that nonexperts have always wanted to know. *Am. J. Neuroradiol.* **39**, 1390–1399. https://doi.org/10.3174/ajnr.A5527 (2018).
12. O'Connor, E. E. & Zeffiro, T. A. Why is clinical fMRI in a resting state?. *Front. Neurol.* **10**, 420. https://doi.org/10.3389/fneur.2019.00420 (2019).
13. Andellini, M., Cannatà, V., Gazzellini, S., Bernardi, B. & Napolitano, A. Test-retest reliability of graph metrics of resting state MRI functional brain networks: A review. *J. Neurosci. Methods* **253**, 183–192. https://doi.org/10.1016/j.jneumeth.2015.05.020 (2015).
14. Bandt, C. & Pompe, B. Permutation Entropy: A Natural Complexity Measure for Time Series. *Phys. Rev. Lett.* **88**, 174102. https://doi.org/10.1103/PhysRevLett.88.174102 (2002).
15. Lehnertz, K. Ordinal methods for a characterization of evolving functional brain networks. *Chaos* **33**, 022101. https://doi.org/10.1063/5.0136181 (2023).
16. Nicolaou, N. & Georgiou, J. Detection of epileptic electroencephalogram based on permutation entropy and support vector machines. *Expert Syst. Appl.* **39**, 202–209. https://doi.org/10.1016/j.eswa.2011.07.008 (2012).
17. Şeker, M., Özbek, Y., Yener, G. & Özerdem, M. S. Complexity of EEG dynamics for early diagnosis of Alzheimer's disease using permutation entropy neuromarker. *Comput. Methods Programs Biomed.* **206**, 106116. https://doi.org/10.1016/j.cmpb.2021.106116 (2021).
18. Kaiser, A. et al. EEG data quality: Determinants and impact in a multicenter study of children, adolescents, and adults with attention-deficit/hyperactivity disorder (ADHD). *Brain Sci.* **11**, 214. https://doi.org/10.3390/brainsci11020214 (2021).
19. Lepping, R. J. et al. Quality control in resting-state fMRI: the benefits of visual inspection. *Front. Neurosci.* **17**, 1076824. https://doi.org/10.3389/fnins.2023.1076824 (2023).

20. Salinsky, M. C., Oken, B. S. & Morehead, L. Test-retest reliability in EEG frequency analysis. *Electroencephalogr. Clin. Neurophysiol.* **79**, 382–392. https://doi.org/10.1016/0013-4694(91)90203-G (1991).
21. Cannon, R. L. et al. Reliability of quantitative EEG (qEEG) measures and LORETA current source density at 30 days. *Neurosci. Lett.* **518**, 27–31. https://doi.org/10.1016/j.neulet.2012.04.035 (2012).
22. Põld, T., Päeske, L., Hinrikus, H., Lass, J. & Bachmann, M. Long-term stability of resting state EEG-based linear and nonlinear measures. *Int. J. Psychophysiol.* **159**, 83–87. https://doi.org/10.1016/j.ijpsycho.2020.11.013 (2021).
23. Popov, T. et al. Test-retest reliability of resting-state EEG in young and older adults. *Psychophysiology* **60**, e14268. https://doi.org/10.1111/psyp.14268 (2023).
24. Babayan, A. et al. A mind-brain-body dataset of MRI, EEG, cognition, emotion, and peripheral physiology in young and old adults. *Sci. Data* **6**, 180308. https://doi.org/10.1038/sdata.2018.308 (2019).
25. Ricci, L. & Perinelli, A. Estimating permutation entropy variability via surrogate time series. *Entropy* **24**, 853. https://doi.org/10.3390/e24070853 (2022).
26. Perinelli, A., Assecondi, S., Tagliabue, C. F. & Mazza, V. Power shift and connectivity changes in healthy aging during resting-state EEG. *Neuroimage* **256**, 119247. https://doi.org/10.1016/j.neuroimage.2022.119247 (2022).
27. R project webpage: https://www.r-project.org/. Accessed October 2024.
28. Nicolaou, N. & Georgiou, J. The use of permutation entropy to characterize sleep electroencephalograms. *Clin. EEG Neurosci.* **42**, 24–28. https://doi.org/10.1177/155005941104200107 (2011).
29. Li, J., Yan, J., Liu, X. & Ouyang, G. Using permutation entropy to measure the changes in EEG signals during absence seizures. *Entropy* **16**, 3049–3061. https://doi.org/10.3390/e16063049 (2014).
30. Jordan, D., Stockmanns, G., Kochs, E., Pilge, S. & Schneider, G. Electroencephalographic order pattern analysis for the separation of consciousness and unconsciousness. *Anesthesiology* **109**, 1014–1022. https://doi.org/10.1097/aln.0b013e31818d6c55 (2008).
31. Keller, K., Unakafov, A. & Unakafova, V. Ordinal patterns, entropy, and EEG. *Entropy* **16**, 6212–6239. https://doi.org/10.3390/e16126212 (2014).
32. Barry, R. J. & De Blasio, F. M. EEG differences between eyes-closed and eyes-open resting remain in healthy ageing. *Biol. Psychol.* **129**, 293. https://doi.org/10.1016/j.biopsycho.2017.09.010 (2017).
33. Quintero-Quiroz, C. et al. Differentiating resting brain states using ordinal symbolic analysis. *Chaos* **28**, 106307. https://doi.org/10.1063/1.5036959 (2018).
34. Masoller, C. et al. Quantifying sudden changes in dynamical systems using symbolic networks. *New J. Phys.* **17**, 023068. https://doi.org/10.1088/1367-2630/17/2/023068 (2015).
35. Vecchio, F. et al. Entropy as measure of brain networks' complexity in eyes open and closed conditions. *Symmetry* **13**, 2178. https://doi.org/10.3390/sym13112178 (2021).
36. Brunner, C., Billinger, M., Seeber, M., Mullen, T. R. & Makeig, S. Volume conduction influences scalp-based connectivity estimates. *Front. Comput. Neurosci.* **10**, 121 https://doi.org/10.3389/fncom.2016.00121 (2016).
37. Van de Steen, F. et al. Critical comments on EEG sensor space dynamical connectivity analysis. *Brain Topogr.* **32**, 643. https://doi.org/10.1007/s10548-016-0538-7 (2019).
38. Cao, Y., Tung, W.-W., Gao, J. B., Protopopescu, V. A. & Hively, L. M. Detecting dynamical changes in time series using the permutation entropy. *Phys. Rev. E* **70**, 046217. https://doi.org/10.1103/PhysRevE.70.046217 (2004).
39. Amigó, J. M., Keller, K. & Unakafova, V. A. Ordinal symbolic analysis and its application to biomedical recordings. *Philos. Trans. R. Soc. A Math. Phys. Eng. Sci.* **373**, 20140091. https://doi.org/10.1098/rsta.2014.0091 (2015).
40. Kreuzer, M., Kochs, E. F., Schneider, G. & Jordan, D. Non-stationarity of EEG during wakefulness and anaesthesia: Advantages of EEG permutation entropy monitoring. *J. Clin. Monit. Comput.* **28**, 573–580. https://doi.org/10.1007/s10877-014-9553-y (2014).
41. Kottlarz, I. et al. Extracting robust biomarkers from multichannel EEG time series using nonlinear dimensionality reduction applied to ordinal pattern statistics and spectral quantities. *Front. Physiol.* **11**, 614565. https://doi.org/10.3389/fphys.2020.614565 (2021).
42. Labate, D., La Foresta, F., Morabito, G., Palamara, I. & Morabito, F. C. Entropic measures of EEG complexity in Alzheimer's disease through a multivariate multiscale approach. *IEEE Sens. J.* **13**, 3284–3292. https://doi.org/10.1109/jsen.2013.2271735 (2013).
43. Kalpakis, K. et al. Permutation entropy analysis of vital signs data for outcome prediction of patients with severe traumatic brain injury. *Comput. Biol. Med.* **56**, 167–174. https://doi.org/10.1016/j.compbiomed.2014.11.007 (2015).
44. Ouyang, G., Dang, C., Richards, D. A. & Li, X. Ordinal pattern based similarity analysis for EEG recordings. *Clin. Neurophysiol.* **121**, 694–703. https://doi.org/10.1016/j.clinph.2009.12.030 (2010).
45. Yang, Y. et al. Epileptic seizure prediction based on permutation entropy. *Front. Comput. Neurosci.* **12**, 55. https://doi.org/10.3389/fncom.2018.00055 (2018).
46. Bratu, I. F. et al. Permutation entropy-derived parameters to estimate the epileptogenic zone network. *Epilepsia* **65**, 389–401. https://doi.org/10.1111/epi.17849 (2023).
47. Olofsen, E., Sleigh, J. W. & Dahan, A. Permutation entropy of the electroencephalogram: A measure of anaesthetic drug effect. *Br. J. Anaesth.* **101**, 810–821. https://doi.org/10.1093/bja/aen290 (2008).
48. Harris, B. The statistical estimation of entropy in the non-parametric case. *Top. Inf. Theory* **16**, 323–355 (1975).
49. Ricci, L., Perinelli, A. & Castelluzzo, M. Estimating the variance of Shannon entropy. *Phys. Rev. E* **104**, 024220. https://doi.org/10.1103/PhysRevE.104.024220 (2021).
50. Meghdadi, A. H. et al. Resting state EEG biomarkers of cognitive decline associated with Alzheimer's disease and mild cognitive impairment. *PLoS ONE* **16**, 1–31. https://doi.org/10.1371/journal.pone.0244180 (2021).
51. LEMON public database URL: https://fcon_1000.projects.nitrc.org/indi/retro/MPI_LEMON.html. (2019).
52. Perinelli, A., Castelluzzo, M., Tabarelli, D., Mazza, V. & Ricci, L. Relationship between mutual information and cross-correlation time scale of observability as measures of connectivity strength. *Chaos* **31**, 073106. https://doi.org/10.1063/5.0053857 (2021).
53. Glasser, M. F. et al. A multi-modal parcellation of human cerebral cortex. *Nature* **536**, 171–178. https://doi.org/10.1038/nature18933 (2016).
54. Miller, G. Note on the bias of information estimates. *Information theory in Psychology: Problems and methods* 95–100 (1955).
55. Schreiber, T. & Schmitz, A. Surrogate time series. *Physica D* **142**, 346–382. https://doi.org/10.1016/S0167-2789(00)00043-9 (2000).
56. Schreiber, T. & Schmitz, A. Improved surrogate data for nonlinearity tests. *Phys. Rev. Lett.* **77**, 635–638. https://doi.org/10.1103/PhysRevLett.77.635 (1996).
57. Ricci, L., Castelluzzo, M., Minati, L. & Perinelli, A. Generation of surrogate event sequences via joint distribution of successive inter-event intervals. *Chaos* **29**, 121102. https://doi.org/10.1063/1.5138250 (2019).

Author contributions

The authors contributed equally to this work. All authors have read and agreed to the published version of the manuscript.

Declarations

Competing interests
The authors declare no competing interests.

Ethics approval
EEG data used in the present work belong to the Leipzig Mind-Brain-Body "LEMON" database, for which the related study protocol was approved by the ethical committee at the University of Leipzig (reference number 154/13-ff)[24].

Additional information
Correspondence and requests for materials should be addressed to A.P. or L.R.

Reprints and permissions information is available at www.nature.com/reprints.

Publisher's note Springer Nature remains neutral with regard to jurisdictional claims in published maps and institutional affiliations.